Kinetics and morphological characteristics of struvite (MgNH4PO4.6H2O) under the influence of maleic acid

by Athanasius Bayuseno

Submission date: 28-Aug-2021 01:04AM (UTC+0700)
Submission ID: 1636971042
File name: 1-s2.0-S2405844020303789-main.pdf (1.73M)
Word count: 6854
Character count: 34995

Heliyon 6 (2020) e03533

Contents lists available at ScienceDirect

Heliyon

journal homepage: www.cell.com/heliyon

Research article

Kinetics and morphological characteristics of struvite ($MgNH_4PO_4.6H_2O$) under the influence of maleic acid

Athanasius Priharyoto Bayuseno [a,*], Dyah Suci Perwitasari [b], Stefanus Muryanto [c], Mohammad Tauviqirrahman [a], Jamari Jamari [a]

[a] Department of Mechanical Engineering, Diponegoro University, Tembalang Campus, Semarang 50275, Indonesia
[b] Department of Chemical Engineering, Universitas Pembangunan National "Veteran" Jawa Timur, Surabaya 60294 Indonesia
[c] Department of Chemical Engineering, UNTAG University in Semarang, Bendhan Dhuwur Campus, Semarang 50233, Indonesia

ARTICLE INFO

Keywords:
Materials chemistry
Physical chemistry
Kinetics
Maleic acid
Struvite
Struvite-(K)

ABSTRACT

This work reports a stirred-batch lab crystallization to examine the influence of maleic acid ($HO_2CCHCHCO_2H$), and temperatures (30 and 40 °C) on crystallization kinetics and morphology of struvite. The crystallization was followed by measuring the pH change up to 70 min. The pH decreased drastically for the first 5 min of the run, then started to tail off. It was found that the crystallization rate constants range from 1.608 to 6.534 per hour, which agrees with the most published value. Higher maleic acid concentrations resulted in greater growth retardation; the highest retardation was 74.21%, which was achieved for 30 °C with 20.00 ppm maleic acid. SEM imaging of the obtained precipitates showed irregular prismatic morphology, and the associated EDX confirmed that the precipitates were struvite ($MgNH_4PO_4{\cdot}6H_2O$). As checked through XRD, the crystalline nature of the struvite was further confirmed, and that co-precipitation of struvite with struvite-K was observed. The co-precipitation was the result of K^+ adsorption onto the crystal surface. Temperatures had less influence on struvite crystallization. At 40°C and 20.00 ppm the rate constant was 1.332 per hour; whereas at 30°C and 0.00 ppm) the corresponding was 1.776 per hour, indicating the retardation of about 25%. Thus, the temperature effect is only 1/3 of the maleic acid effect. The current findings suggest that the presence of maleic acid can be used to elucidate the mechanism of crystallization as well as the crystalline phase transformation of struvite. In practical terms, maleic acid could be potential as a scale inhibitor.

1. Introduction

Scale formation of struvite ($MgNH_4PO_4{\cdot}6H_2O$) is frequently found in wastewater treatment (WWT) plant facilities, e.g. the anaerobic treatment of piggery and poultry wastes and wine distillery effluents, since the wastes generally contain significant amounts of Mg^{2+}, NH_4–N, and PO_4^{-2}, the forming components of struvite [1]. The scaling is especially prevalent in points where turbulent flows occur, rendering the solution to become alkaline due to the release of CO_2 from the solution [2, 3]. The struvite scale formation can be uncontrollable and massive which results in clogging pumps and other process equipment, blocking the piping system, and hence in reduction of energy and material transfer. In some cases the excessive scale growth may lead to the total breakdown of the processing facilities causing substantial financial losses.

On the other hand, since ammonium and phosphate ions are essential for plant growth, struvite is considered potential as a fertilizer. In fact, recovery of Mg^{2+}, NH_4–N, and PO_4^{-2} from wastewater as struvite has been an area of promising enterprise since the crystals produced are regarded as superior due to their slow-release nature [4, 5, 6]. Another important area of struvite research is the presence of this phosphate material as one of the major components of infectious urinary stones [7, 8]. This paper, however, discusses an investigation on struvite crystallization in an attempt to alleviate the burden of scaling problem encountered by many industries and WWT services. Struvite precipitation, or struvite crystallization, as the term interchangeably used, has been widely practiced for the removal of environmentally harmful ammonium nitrogen (NH_4–N) and phosphorus (PO_4^-) from WWT, since it is highly efficient, simple and environmentally sustainable [9, 10].

Scale formation of struvite is initiated by crystallization, a process which is significantly subject to a number of physical-chemical parameters. Among these parameters are pH level of the solution [1, 11, 12], and the presence of foreign ions [2, 3, 12].

* Corresponding author.
E-mail address: apbayuseno@gmail.com (A.P. Bayuseno).

https://doi.org/10.1016/j.heliyon.2020.e03533
Received 19 November 2019; Received in revised form 22 January 2020; Accepted 2 March 2020

1.1. Influence of pH

Throughout the precipitation of struvite, proton (H^+) is released (see Eq.(1)), thus lowering the pH level of the precipitating solution. Therefore, research on struvite precipitation are typically carried out at a certain pH range higher than neutral. Experiments on struvite precipitation at a low pH [13, 14] have shown minimal amounts of crystals obtained, and hence impractical. As can be inferred from Eq. (1), higher alkaline pH is more favorable for the crystallization of struvite. The work of Song et al [15] on struvite, used a pH range from 8.0 to 12.0 and showed that the optimum pH was between 9.5 and 10.5, whereby as much as 93% of phosphates (P) in the original solution was successfully crystallized. However, too high a pH level (>11.0) is counter productive due to the occurrence of side reactions forming $Mg(OH)_2$ and the evolution of free NH_3 [16], thus reducing the Mg^{2+} and NH_4^+ ions available for struvite formation. The availability of Mg^{2+} and PO_4^{-2} for struvite formation is also reduced due to the formation of another magnesium phosphate mineral, namely $Mg_3(PO_4)_2\ 22H_2O$ if the initial pH of the solution is 10.00 or higher [17]. It is argued that the formation of $Mg_3(PO_4)_2\ 22H_2O$ is instigated by the dominant species of PO_4^{-3} in the solution at pH 10.00. In fact, different species of phosphate ions: PO_4^{3-}, HPO_4^{2-}, $H_2PO_4^-$ [16–19] will be dominant in the solution once the pH level changes. Such a change will result in the formation of other phosphate compounds alongside struvite, such as Mg_3PO_4 and $Mg(OH)_2$ [14].

More efficient process can be achieved if the crystallization proceeds in predominantly a heterogeneous mode so that the crystals obtained is relatively large in size and the fines are minimal. As reported [20], the metastable zone of struvite precipitation is between the pH of 8.00 and 10.00.

Theoretically, the rise of pH of a solution increases the ionic activity product (IAP) with the consequence that the supersaturation of the solution will also increase. In this way, the kinetic rates will rise accordingly. Therefore, a slight variation of pH has often been utilized to examine the crystallization kinetics of struvite. As reported by Crutchik and Garrido [16] even for a slight difference in pH of 8.2, 8.5 and 8.8, the kinetic rates of struvite crystallization increase as 1.21 10^{-4}, 1.25 10^{-4}, and 1.63 10^{-4} mol m^{-2} min^{-1}, respectively.

1.2. Influence of additives and impurities

The presence of either additives or impurities, even in ppm amounts, may significantly influence the precipitation of struvite. The effect can be obvious, e.g.on the alteration of morphology [2, 3, 21], crystal phases [3], as well as precipitation rates [22]. Increasing awareness on sustainable practices in industry, which subsequently leads to environmentally friendly methods has encouraged extensive research on struvite precipitation using additives of organic origin. Our work on struvite precipitation [12] has revealed that minute amounts of citric acid (1.00–20.00 ppm) were able to significantly retard the growth of the crystals. The effect, however, was not notably obvious for the change in morphology. The work of Song et al [23] attempted to recover phosphorus (P) from swine wastewater using organic acids. It was found that the P recovery was highest for acetic acid, followed by succinic acid and citric acid, respectively. Additionally, the effect of succinic and citric acids on the morphology of the struvite crystals obtained was negligible.

The current paper reports a stirred-batch lab crystallization to examine the influence of maleic acid ($HO_2CCHCHCO_2H$), one of the environmentally friendly, organic additives, on crystallization kinetics and morphology of struvite ($MgNHPO_4.6H_2O$). Other parameters investigated were the temperature of the crystallization: 30 and 40°C. The pH change of the solution was carefully monitored to establish the kinetics of the precipitation.

2. Materials and methods

In this work the term crystallization is used interchangeably with precipitation.

2.1. Batch crystallization experiments

The crystallization was carried out by mixing 0.11 M $MgCl_2$ and 0.11 M $NH_4H_2PO_4$ solutions, 100 mL each, in a 250 mL beaker. In order to maintain the desired pH level appropriate for struvite precipitation, i.e. 9.00, 1.0 N KOH solution was added drop-wise from a burette. To keep the temperature of the solution constant, the beaker was placed in a thermostatically-controlled water bath. Also, the solution was continuously stirred at a certain speed to keep it homogeneous, but not extremely fast so as to break the forming crystals. A digital pH meter was used to record the pH level uninterruptedly as the precipitation proceeded.

To investigate the effect of maleic acid, crystals of this organic species (in ppm amounts) were diluted with double-distilled water and then the resulting solution was added into the $MgCl_2$ solution. For each run, the volume of the maleic acid solution added into the $MgCl_2$ solution was about 5.0 mL, and thus can be regarded as minimal in comparison to the whole crystallizing solution. Hence, after the addition, the volume of the solution was considered constant.

During the precipitation, the pH level of the solution decreased with time, drastically at the outset, and started to tail off after about 10 min. Hence, 90 min period was considered adequate for a complete precipitation. At the end of the experiment, the stirrer was switched off, and the solution was filtered immediately using ashless Whatmann filter paper to obtain the crystals. Subsequently, the crystals were washed with distilled water to get rid of impurities which could have attached on the crystal surfaces. It was assumed that only chlorides and alkali ions were removed during washing [24]. The wet crystals were air-dried in a secure place for 48 h, and the resulting dry crystals were subsequently stored for characterization.

Further experimental errors in the current experiments have been taken into account according to the methodology that has been implemented for the author's work previously [2, 12] as follows; Firstly, error in weighing the chemicals: $MgCl_2$ and $NH_4H_2PO_4$ have been covered by using an analytical balance with four-digit accuracy i.e. 0.0001 g. This is commonly used in experiments involving chemicals weighing. Secondly, errors in preparing the crystallization solution were also included in standard laboratory glassware with a volumetric accuracy of ±5%. Thirdly, errors in pH measurement were considering using a pH meter with an accuracy of 0.01. The pH measurement results clearly indicated the number presented. Fourthly, weighing of the struvite crystals obtained considered the accuracy of weighing similar to that of the previous chemicals.

2.2. Materials characterization

The mineralogical composition and morphology of the precipitate were acquired by the X-ray powder diffraction (XRPD) method and SEM (scanning electron microscopy) equipped with an energy dispersive X-ray analysis (SEM-EDX), respectively. For that analysis, the solid crystals were initially crushed with a pestle and mortar to yield the particle size <75 μm. This powder was subsequently mounted on the surface of the XRPD aluminum sample holder.

X-ray data for mineralogical composition were recorded by Bragg Brentano X-ray diffractometer (Philips 1830/40). The measurement parameters (5-85^O 2θ, 0.02^O steps, 15 s/step) were selected. Detailed measurements are presented in Table 1. To identify the crystalline phases of the samples a PC-based search-match program (Match software) was used, of which the identified phases were subsequently justified by the Rietveld method [25]. The Rietveld profile was then refined with the Program Fullprof-2k, version 3.30 [26].

The parameters were refined during the running program as follows: (i) the 2θ° scale zero shifting, (ii) the polynomial fitting for the background parameter, (iii) the phase scale factors, (iv) the unit-cell parameters, (v) the peak asymmetry and the peak profile functions. The full-width at half-maximum (FWHM) of x-ray peak profiles as a function of tan (θ) was determined using the u-v-w formula of Caglioti et al. [27],

Table 1. The parameter measurements of the XRPD method.

Geometry	Bragg-Brentano
Goniometer radius	240 mm
Radius source	CuK_{α}
Generator	40 kV, 30 mA
Tube	Normal focus 10 x 1 mm
Divergence and receiving slits	0.2117^{O}
Soller slits	5.3^{O}
Resolving slit	100 mm
Monochromator	Graphite (diffracted beam)
Detector	Scintillation counter
The scan parameters and step size	5 - 85^{O} 2θ in 0.020° increments
Integration time	10 s

where u, v, and w were selected to be values of the measured quartz. The preferred orientation of all crystalline phases was refined during the refinements. The refined values of unit-cell parameters of the crystal structure models and the obtained scale factor of the diffraction intensity were used to calculate weight. % of phase abundance from which were calculated by the program [28]. The strategy for the Rietveld refinements of the crystalline sample has been presented in detail elsewhere [29].

Further, SEM-EDX (JEOL JSM 5200) were employed to examine the morphology and elemental analysis of the crystalline product. Before SEM/EDX analysis, the ground powder was placed with the epoxy on the surface of the Al-sample holder and then sputtered with carbon.

3. Results and discussion

3.1. Kinetics of struvite crystallization

As a concentration-forced process, higher concentrations of reactants accelerate the crystallization reaction. In the crystallization of struvite, the reaction equation is as follows [30]:

$$Mg^{2+} + NH_4^+ + H_2PO_4^- + 6H_2O \rightarrow MgNH_4PO_4{\cdot}6H_2O + 2H^+ \quad (1)$$

As can be seen (Eq (1)), as the struvite crystallization proceeds, H^+ is released. Hence it is possible to relate the reaction rates and their kinetic orders by measuring the change in pH of the solution. In other words, the rate of struvite crystallization can be calculated by measuring the pH change.

Theoretically, the kinetics of a chemical reaction explains that the rate of decrease in the concentration of reactants equals the rate of increase in the concentration of the products. In the crystallization of struvite given previously in Eq. (1), the rate can be mathematically written as [30]:

$$-\frac{d[Mg^{2+}]}{dt} = \frac{1}{2}\frac{[H^+]}{dt} \quad (2)$$

As can be seen (Eq. (2)), during the crystallization of struvite, the amount of Mg^{2+} consumed equals half the increase in $[H^+]$, which in the pH meter reading corresponds the decrease in pH. Hence, obviously, the rate of the struvite crystallization reaction can be calculated by monitoring the pH change.

The left-hand side of Eq. (2) is the same as,

$$-\frac{d[Mg^{2+}]}{dt} = \kappa_{Mg}[Mg^{2+}] \quad \text{or} \quad -\frac{d[Mg^{2+}]}{[Mg^{2+}]} = \kappa_{Mg}dt \quad (3)$$

Equally, for the right-hand side of Eq. (2),

$$\frac{1}{2}\frac{d[H^+]}{dt} = \kappa_H[H^+]\frac{1}{2}\frac{d[H^+]}{dt} \quad \text{or} \quad \frac{1}{2}\frac{d[H^+]}{[H^+]} = \kappa_H dt\frac{1}{2}\frac{d[H^+]}{[H^+]}\kappa_H dt \quad (4)$$

Manipulating Eq. (2), it is possible to combine Eqs. (3) and (4) to yield,

$$-\frac{d[Mg^{2+}]}{[Mg^{2+}]} = \frac{1}{2}\frac{d[H^+]}{dt} \quad (5)$$

$-\frac{d[Mg^{2+}]}{[Mg^{2+}]} = \frac{1}{2}\frac{d[H^+]}{dt}$ Since pH = -log $[H^+]$, Eq. (5) can be integrated as follows

$$-\int_0^t \frac{d[Mg^{2+}]}{[Mg^{2+}]} = \frac{1}{2}\int_0^t \frac{d[H^+]}{[H^+]} \quad (6)$$

Then,

$$\ln[Mg^{2+}]^t = \ln[Mg^{2+}]^0 - \frac{1}{2}\ln\left[\frac{(H^+)^t}{(H^+)^0}\right] \quad (7)$$

or

$$\ln[Mg^{2+}]^t = \ln[Mg^{2+}]^0 - \frac{1}{2}\ln\left[\frac{10^{-pH^t}}{10^{-pH^0}}\right] \quad (8)$$

$$\ln[Mg^{2+}]^t = \ln[Mg^{2+}]^0 - \frac{1}{2}\ln\left[\frac{10^{-pH^t}}{10^{-pH^0}}\right] \quad \text{or} \quad [Mg^{2+}]^t = \exp\left[\ln(Mg^{2+})_0 - \frac{1}{2}\left(\frac{10^{-pH_t}}{10^{-pH_0}}\right)\right] \quad (9)$$

Using (Eq (9)) the amount of magnesium ions left in the crystallizing solution at any time **t**, i.e. $[Mg^{2+}]^t$ was calculated based on the pH reading. Subsequently, the $[Mg^{2+}]$ data is used to solve the kinetic and the rate of the crystallization.

A typical recorded pH values which were converted into $[Mg^{2+}]$ were tabulated as shown in Table 2.

A number of researchers confirmed that crystallization of struvite follows first order kinetics [1, 2, 31, 32]. Hence, an attempt was made to fit the results of the current work in first order kinetics. The kinetic model correlates the decrease of a reactant (–dC/dt) to the rate constant (k) and the reactant concentration at time t (C) minus the reactant concentration at equilibrium (C_{eq}), as presented in Eq. (10).

Table 2. Recorded pH and its associated $[Mg^{2+}]$ at 30°C, with 0.00 and 20.00 ppm maleic acid.

Time, min	Recorded pH		$[Mg^{2+}]$, molar	
	0.00 ppm	20.00 ppm	0.00 ppm	20.00 ppm
1	9.00	9.00	0.113077	0.113077
2	8.99	8.93	0.110473	0.094933
3	8.98	8.93	0.107871	0.094933
4	8.97	8.93	0.105272	0.094933
5	8.95	8.92	0.100088	0.092370
10	8.94	8.91	0.097506	0.089819
15	8.94	8.91	0.097506	0.089819
20	8.93	8.90	0.094933	0.087282
25	8.93	8.90	0.094933	0.087282
30	8.93	8.90	0.094933	0.087282
35	8.92	8.89	0.092370	0.084760
40	8.92	8.89	0.092370	0.084760
45	8.92	8.87	0.092370	0.079767
50	8.91	8.87	0.089819	0.079767
55	8.91	8.87	0.089819	0.079767
60	8.90	8.86	0.087282	0.077299
65	8.90	8.84	0.087282	0.072431
70	8.89	8.84	0.084760	0.072431

$$-\frac{dC}{dt} = \kappa(C - C_{eq}) \quad (10)$$

The linearized form of Eq. (10) is:

$$\ln(C - C_{eq}) = -\kappa t + \ln(C_0 - C_{eq}) \quad (11)$$

where,

C = $[Mg^{2+}]$ at any time, t, (molar),
Ceq = $[Mg^{2+}]$ at equilibrium, (molar),
Co = initial $[Mg^{2+}]$ at zero time, (t = 0), (molar),
k = reaction rate constant, (h^{-1}),
t = crystallization time, (min.).

Figure 1 shows the experimental data at a lower temperature tested, i.e. 30°C. As can be seen (Figure 1 (a)), the pH of the solution drops drastically at the start of the run, namely for the first 5 min. Afterwards the decrease is relatively gradual, and tails off after about 70 min. As can be seen in Figure 1 (b), a plot of ln(C-C_{eq}) against time **t** for the first 5 min yields a straight line with slope – k, which is the rate constant for the reactions. Figure 1(b) demonstrates clearly that the experimental data fit the first order kinetic significantly (R^2 = 0.9938), the slope, k = 0.1089 and thus the calculated rate constant is 6.534 per hour. This value is in the range of rate constants commonly found in struvite crystallization [1, 32, 33, 34]. Kinetic order plotting similar to Figure 1b (not shown) was carried out for all experimental data, i.e. for 1.00, 10.00, and 20.00 ppm of maleic acid tested, and the resulting rate constants are depicted in Table 3. As can be seen, both the first period of precipitation (0–5 min) and the second (10–70 min) relatively fit the kinetic order selected, namely the first order. Attempts were made to fit for other kinetic models on struvite crystallization as reported by other researchers: pseudo-first order [4], pseudo-second order [4], and second order [21, 34, 35], but all resulting in a poorer match. The third order kinetic model was also tried [36] but with even worse results. Therefore, it was concluded that the first order kinetics are more justifiable for the current work, which is also widely confirmed by other investigators as previously cited.

The current work indicates that the maleic acid influence on the kinetic parameters seems to be inconsistent when the amount of the acid exceeds 10.00 ppm (Table 3). This would require further substantiation in our future projects. Thus, the maleic acid effects should be cautiously scrutinized. Overall, however, it can be clearly seen that a pattern has emerged, i.e. the pH drop was sharp in the first 5 min of the runs, and subsequently levelled off (Figure 1a); the manipulation/calculation of which is presented previously (Table 2). The typical pH drop is widely recognized in struvite precipitation from solution under the influence of additives [1, 2, 22, 30, 37].

As regards the temperature examined, higher temperature (= 40°C) results in lower rate constants, indicating a decrease in the reaction rates (Figure 2a,b) (Table 3). The higher temperatures of up to 40°C would cause higher solubility with the implication that struvite is more difficult to precipitate [30, 37], therefore decreasing the reaction rate. Additionally, in the crystallization of struvite, temperature may affect the

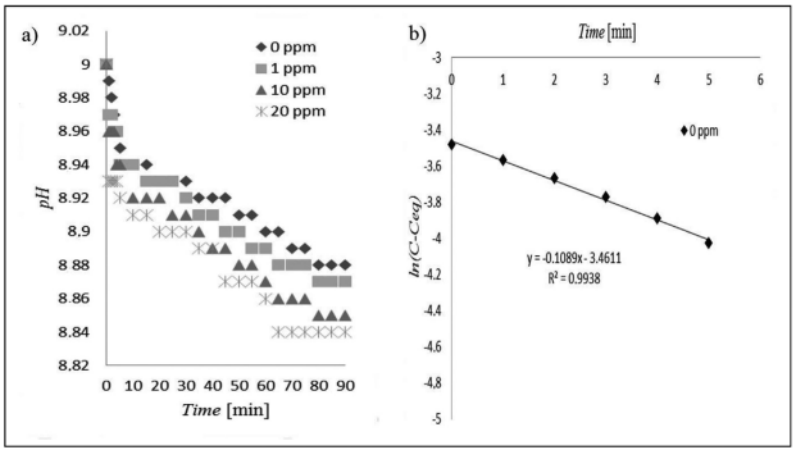

Figure 1. Struvite crystallization at 30 °C with and without maleic acid; (a) pH reduction profile; (b) fit of first order kinetic without maleic acid. C = $[Mg^{2+}]$ at time t; Ceq = $[Mg^{2+}]$ at equilibrium, i.e. when the crystallization was completed.

Table 3. Kinetic parameters of struvite crystallization.

	The first period (0–5 min)		The second period (10–70 min)	
Amount of Maleic acid	First order kinetic parameter (h^{-1})	R^2	First order kinetic parameter (h^{-1})	R^2
Stirring speed of 300 rpm and T = 30 °C				
0 ppm	6.534	0.9938	1.776	0.9452
1 ppm	5.586	0.8714	1.614	0.9443
10 ppm	5.544	0.8116	1.614	0.9223
20 ppm	6.102	0.8534	1.608	0.8888
Stirring speed of 300 rpm and T = 40 °C				
0 ppm	5.166	0.9922	1.698	0.9656
1 ppm	4.626	0.8872	1.548	0.9320
10 ppm	4.086	0.8949	1.278	0.9602
20 ppm	4.698	0.8150	1.332	0.9400

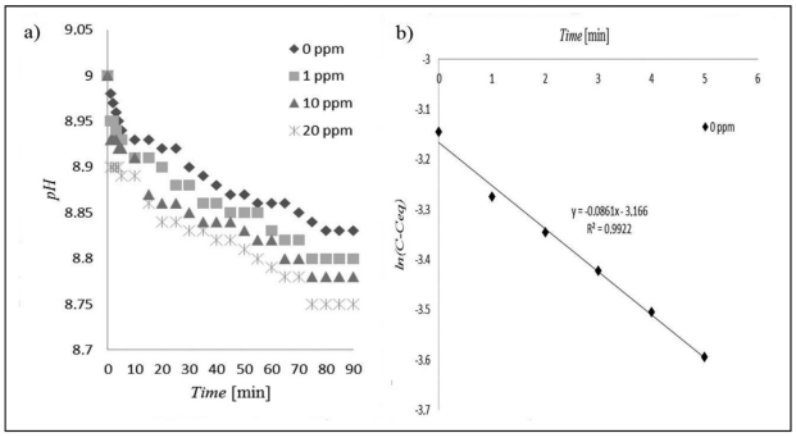

Figure 2. Struvite crystallization at 40 °C with and without maleic acid; (a) pH reduction profile; (b) fit of first order kinetic without maleic acid. C = $[Mg^{2+}]$ at time t; Ceq = $[Mg^{2+}]$ at equilibrium, i.e. when the crystallization was completed.

relative rates of both diffusion and surface integration of crystal growth units [38]. In this current work, it is assumed that the temperatures may affect the rates in a negative manner.

In the absence of maleic acid the rate constants were 6.534 and 5.166 per hour for 30 °C and 40 °C, respectively. However, at the same temperature level but in the presence of highest concentration of maleic acid, i.e.20.00 ppm, these rate constants were 6.102 and 4.698 per hour, respectively. The percentage of the decrease is therefore (6.534–6.102) × 100 % = 43.2 %, for the condition without maleic acid. Similarly, the decrease under the influence of 20.00 ppm maleic acid = (5.166–4.698) × 100% = 46.8 %. Thus, it can be concluded that the effect of temperature on struvite growth retardation is minimal, i.e. 46.8%–43.2%, or only about 4.00%. Similar findings of the mild effect of temperature on struvite reaction rates were reported by Fang et al [11], where a temperature rise from 21°C to 49°C was only capable of increasing the average crystal size of struvite from 65 μm to 69 μm, an almost negligible increase.

In term of accuracy in the kinetic model used for the study, a further comparison of the author's model with another model used in practice for struvite precipitation was included and some of the published paper has been cited (see-Nelson et al, 2003 [1]; Prywer et al, 2012 [8]; Darwish et al, 2017 [9]; Ali and Schneider, 2006 [20]; Kofina et al, 2007 [21]; Le Corre, 2006 [30]). In fact, the variable uncertainties and significant numbers as presented in this current work are consistent with those published in those papers. Therefore, it was affirmed that the present study is consistent in terms of accuracy with the work of other prominent researchers in this area of struvite crystallization, especially when the batch mode of crystallization was performed.

3.2. Mineralogical quantitative and morphology analysis of products

In this work, as shown by the XRD analysis, struvite-(K) was found. The formation of the K-doped struvite may be the result of KOH addition for pH adjustment, of which the K^+ adsorbed/incorporated into the struvite. Values of pH in the range of 9.0–10.5 were reported to favor struvite-(K) precipitation during the phosphate and potassium recovery [4, 18].

The kinetic analysis of the precipitating solids has been demonstrated previously (Figures 1 and 2) that two steps of precipitation occurred in the solution at the temperature of 30 and 40 °C. This suggests that two phases are formed during crystallization. The precipitation per second does not proceed in two stages. However, the decrease in pH level does proceed in two distinctive stages, with the first stage (0–5 min) the pH drops rather steeply; and the second one decreases gradually. This suggests by the XRPD and SEM/EDX analysis. The XRPD Rietveld analysis validated two phases of the struvite and struvite-(K) formed in the solution at 30 °C and without maleic acid (Figure 3a). Here, the XRPD peak

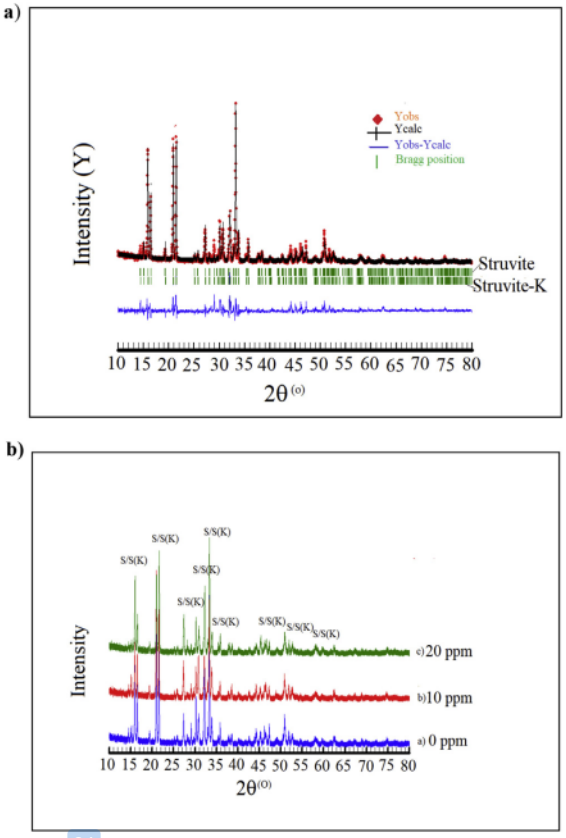

Figure 3. a) XRPD Rietveld refinement plot of the precipitates in the solution at 30°C without maleic acid; b) XRPD patterns of all samples with 0, 10, and 20 ppm maleic acid. The peaks are labelled S (struvite); S(K) (struvite-K).

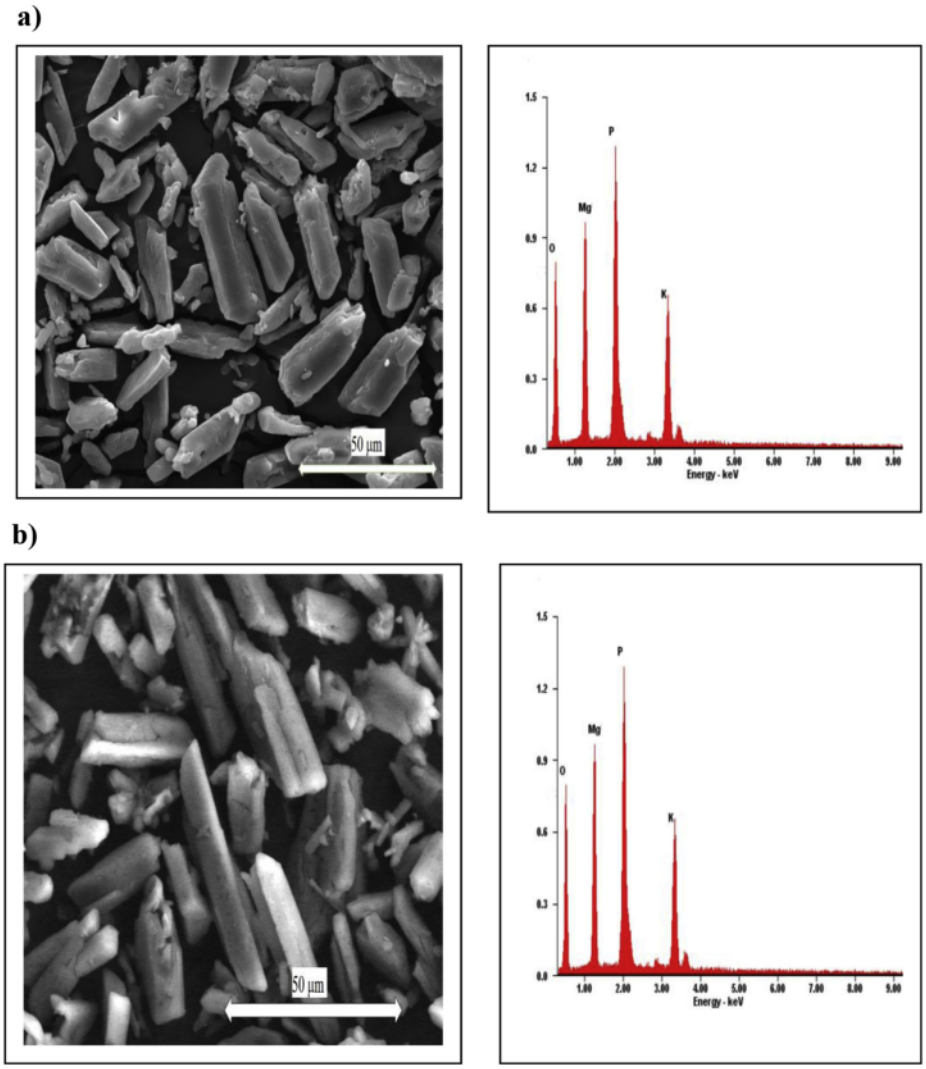

Figure 4. SEM and EDX image of a prismatic shaped crystal morphology obtained from the solution in the presence of a) 0 ppm; b) 20 ppm maleic acid at 30 °C.

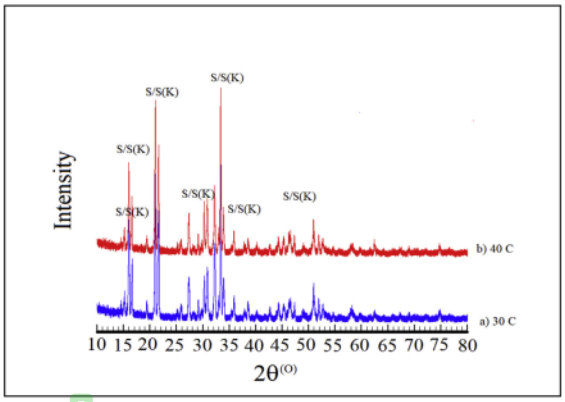

Figure 5. XRPD patterns of the precipitating solid from the solution with 20 ppm maleic acid and temperatures of 30 and 40 °C.

profiles of struvite and struvite-(K) minerals agreed very well with the calculated diffractogram from the crystal structure model [38, 39]. Obviously, all profiles of X-ray spectra could be matched with the model. The XRPD method also confirmed that the precipitates are composed of crystalline structure assuming no amorphous phase, because of no observed hump in the background profile.

Further, XRPD peak profiles of the solids precipitated in the solution with varying maleic acid concentrations are presented in Figure 3b. Each peak profile had been justified by the Rietveld refinement and matched by struvite and struvite-(K). It has been confirmed here that the phase composition of the solid crystal was not altered under influence of maleic acid additive. However, since the minerals form a solid solution, the composition of any single crystal would be a mixture. Figure 4 shows the type of struvite crystal morphology without and with 20 ppm maleic acid additive at the temperature of 30 °C. Irregular prismatic crystal morphology is shown in the SEM images with a size of about 100 µm in length and 10 µm in width, whereas the addition of 20 ppm maleic acid decreased the crystal size (Figure 4). Additionally, the formation of

struvite and struvite-(K) structures could be also confirmed by EDX spectra consisting of K^{+}, Mg^{2+}, O^{2-} and P^{5+} ions.

Likewise, the overlapped peaks of struvite and struvite-(K) could be observed in the XRPD diffractogram of the crystalline solid obtained at the solution temperature of 40 °C (Figure 5), while typical irregular flake-shaped morphology could be obtained, though it is not shown. With increasing temperature, phase compositions of the crystalline solid remained stable, because the chemical equilibrium of MAP ions had been achieved in the solution.

Further, SEM examination confirmed the irregular prismatic-like morphology, which is a typical struvite crystal (30 μm in length and width of 5 μm (Figure 6). This crystal was obtained when 20 ppm maleic acid was added at the temperature of 30 °C. The morphology of crystals has the surface of crystals with quite smooth. It is likewise confirmed that synthesis at 40 °C did not alter the morphology of the struvite obtained. However, a further research should be subjected for obtaining the maximum impact of maleic acid on the phosphate and potassium recovery and morphology. For the establishment and production of struvite a design reactor may be required, in which crucial parameters such as level of supersaturated conditions, pH, temperature, and amount of organic additives can be accurately controlled. Further, the content of struvite and struvite-(K) formed in the solution under the influence of maleic acid was also quantitatively examined by the XRPD Rietveld method. Here the quantitative values (wt. %) was obtained by the XRPD Rietveld analysis using the refined unit cell parameter of each mineral, in which the parameter has been refined by least-square analysis and the refined results were in a reasonable agreement with the published data [38, 39]. With no additive used, the major phase of struvite-(K) (72.9 wt. %) and the minor struvite (27.1 wt. %) was obtained (Figure 7). In the absence of maleic acid, the PO_4^{3-} activity may have a greater effect on struvite-(K) precipitation, which is also controlled by the pH solution through KOH addition. Apparently, a proportion of struvite and

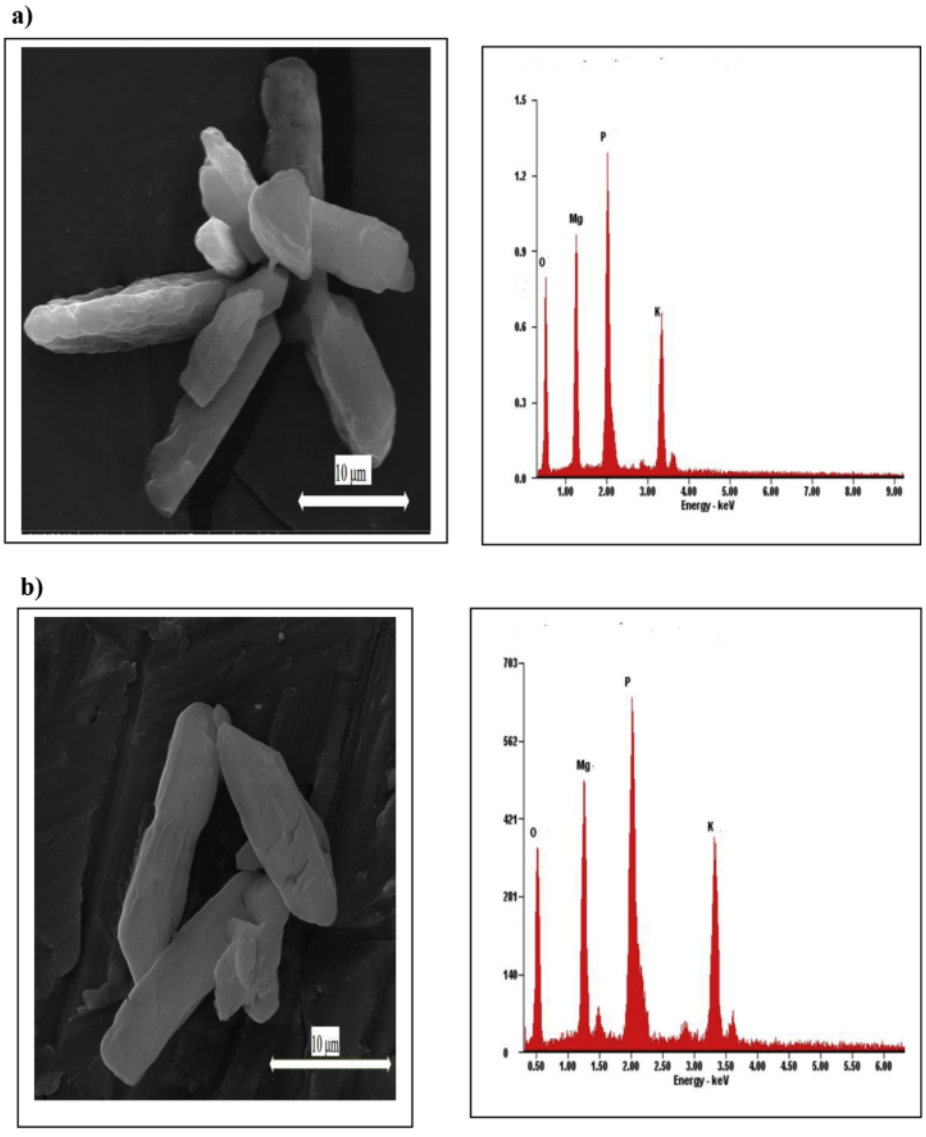

Figure 6. SEM images of morphology for precipitating solids from the solution with 20 ppm maleic acid and temperatures of a) 30 °C; and b) 40 °C.

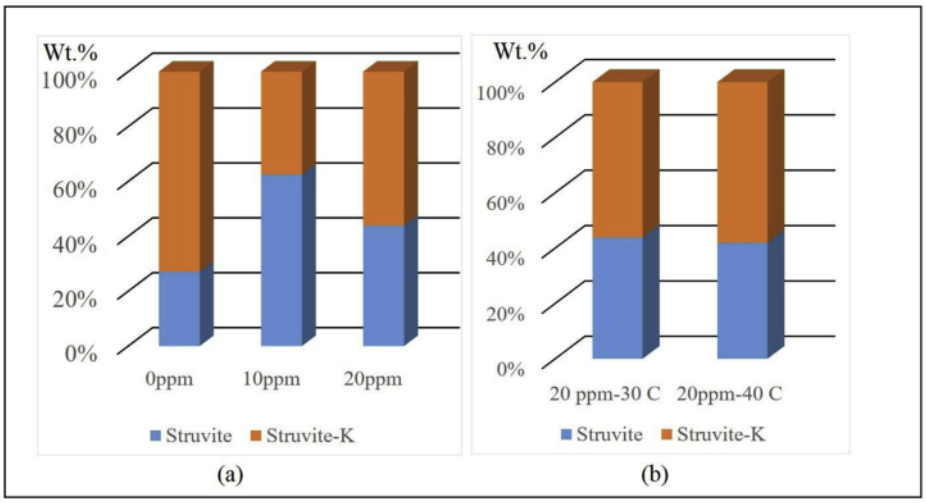

Figure 7. Mineralogical composition of the solid crystals from the solution with a) maleic acid additive (0, 10, and 20 ppm) at a temperature of 30 °C; b) varying temperature and 20 ppm maleic acid.

struvite-(K) could be adjusted by varying in pH solution, whereas the pH values in the range of 9–10.5 are considered optimal for phosphate and potassium recovery [40].

Conversely, an increased content of struvite was obtained as a result of 10 ppm maleic acid additive, then its content reduced because of the addition of 20 ppm maleic acid. Struvite-(K) becomes yet major mineral at this condition. In this way, the less concentration of ammonium ($NH4+$) and the higher PO_4^{3-}activity may occur, once the struvite-(K) crystal had generated. With 20 ppm additive at a temperature of 40 °C, the phase of struvite-(K) (58 wt. %) became the dominant phase in the crystallized solids. This is a positive impact on the recovery of phosphate and potassium in the wastewater treatment industry. However, an increasing temperature did not change significantly in the amounts of struvite-(K) formed. It is suggested here that the lower concentration of maleic acid (<10 ppm) may provide the best removal of ammonium and phosphate through struvite precipitation. Conversely, the absence of maleic acid makes a better condition of phosphate and potassium recoveries in the struvite-(K) crystallization [41, 42, 43, 44].

4. Conclusions

An innovative method was successfully developed to investigate the crystallization kinetics and morphology of struvite, a phosphate mineral that frequently forms a tenacious scale of industrial equipment. This method used the change of pH in the crystallizing solution to calculate the kinetic rates. It was confirmed that this method yielded experimental data compared to conventional practice.

The crystallization process of struvite in this investigation followed two patterns of pH change: a drastic decrease at the start, followed by a gradual decline until the end of the experimental runs. Both patterns appropriately fit the first-order kinetics. The struvite crystallization rates were inhibited by maleic acid even when this acid was present in minute amounts (1.00–20.00 ppm), with the rate constants dropping steadily the higher the maleic acid concentrations added. The rate constants range from 6.534 h^{-1} to 1.332 h^{-1}, which correspond well with published values. A slight discrepancy in the calculated rate constant was discovered when the maleic acid used approaching 20.00 ppm, but the general pattern of the change in rate constants remains. This minor variation could be due to the experimental conditions. Overall, the inhibition of the growth of struvite using maleic acid, within the constraints of this work, is about 47%.

On the other hand, the effect of temperature on the struvite crystal growth is less obvious. Raising the crystallization temperature from 30 °C (without maleic acid) to 40 °C (with the addition of 20.00 ppm maleic acid), resulting in an increase in the inhibition capability by merely 4.00%.

The precipitation in the K-Mg-NH_3-PO_4 system could be confirmed here using the XRPD Rietveld method. Obviously, struvite and struvite-(K) controlled the MAP ion recovery out of the solution at the temperatures of 30 and 40 °C and initial pH 9. The phase abundance of struvite and struvite-(K) could be pH dependence and controlled by maleic acid in the solution. The crystals precipitated from the solution in the absence and presence of maleic acid have the same morphology with the irregular prismatic shape. The differences in crystal sizes could be observed. Shorter and slimmer crystals were developed when the maleic acid was added to the solution.

Declarations

Author contribution statement

Athanasius Bayuseno: Conceived and designed the experiments; Performed the experiments; Wrote the paper.

Dyah Suci Perwitasari: Conceived and designed the experiments; Performed the experiments.

Stefanus Muryanto: Conceived and designed the experiments; Analyzed and interpreted the data; Wrote the paper.

Mohammad Tauviqirrahman: Performed the experiments.

Jamari Jamari: Performed the experiments; Wrote the paper.

Funding statement

Dyah Suci Perwitasari was supported by the University of Pembangunan National, Surabaya Indonesia and Diponegoro University, Semarang.

Competing interest statement

The authors declare no conflict of interest.

Additional information

No additional information is available for this paper.

Acknowledgements

This research was supported by Diponegoro University, Semarang, Indonesia.

References

[1] N.O. Nelson, R.L. Mikkelsen, D.L. Hesterberg, Struvite precipitation in anaerobic swine lagoon liquid: effect of pH and Mg: P ratio and determination of rate constant, Bioresour. Technol. 89 (2003) 229–236.
[2] S. Muryanto, A.P. Bayuseno, Influence of Cu^{2+} and Zn^{2+} as additives on crystallization kinetics and morphology of struvite, Powder Technol. 253 (2014) 602–607.
[3] H. Saidou, A. Korchef, S.B. Moussa, M.B. Amor, Study of Cd^{2+}, Al^{3+}, and SO_4^{2-} ions influence on struvite precipitation from synthetic wastewater by dissolved CO_2 degasification technique, Open J. Inorg. Chem. 5 (2015) 41–51.
[4] T. Zhang, Q. Wang, Y. Deng, R. Jiang, Recovery of phosphorus from swine manure by ultrasound/H_2O_2 digestion, struvite crystallization, and ferric oxide hydrate/biochar adsorption, Front. Chem. 6 (2018) 464–478.
[5] T. Zhang, C. Fang, P. Li, R.F. Jiang, Application of struvite process for nutrient recovery from anaerobic digesters of livestock wastewater, Environ. Protect. Eng. 40 (2014) 29–42.
[6] Y. Jin, Z. Hu, Z. Wen, Enhancing anaerobic digestibility and phosphorus recovery of dairy manure through microwave-based thermochemical pretreatment, Water Res. 43 (2009) 3493–3502.
[7] R. Flannigan, W.H. Choy, B. Chew, D. Lange, Renal struvite stones – pathogenesis, microbiology, and management strategies, Nat. Rev. Urol. 11 (2014) 333–341.
[8] J. Prywer, A. Torzewska, T. Plocinski, Unique surface and internal structure of struvite crystals formed by *Proteus mirabilis*, Urol. Res. 40 (2012) 699–707.
[9] M. Darwish, A. Aris, M.H. Puteh, M.N.H. Jusoh, A.A. Kadir, Waste bones ash as an alternative source of P for struvite precipitation, J. Environ. Manag. 203 (2) (2017) 861–866.
[10] G. Kurtulus, A.C. Tas, Transformations of neat and heated struvite ($MgNH_4PO_4.6H_2O$), Mater. Lett. 65 (2011) 2883–2886.
[11] C. Fang, T. Zhang, R. Jiang, H. Ohtake, Phosphate enhance recovery from wastewater by mechanism analysis and optimization of struvite settleability in fluidized bed reactor, Sci. Rep. 6 (2016) 32215.
[12] D.S. Perwitasari, L. Edahwati, S. Sutiyono, S. Muryanto, J. Jamari, A.P. Bayuseno, Phosphate recovery through struvite-family crystals precipitated in the presence of citric acid: mineralogical phase and morphology evaluation, Environ. Technol. 38 (2017) 2844–2855.
[13] C.-C. Wang, X.-D. Hao, G.-S. Guo, M.C.M. van Loosdrecht, Formation of pure struvite at neutral pH by electrochemical deposition, Chem. Eng. J. 159 (2010) 280–283.
[14] X.D. Hao, C.C. Wang, L. Lan, M.C.M. van Loosdrecht, Struvite formation, analytical methods and effects of pH and Ca^{2+}, Water Sci. Technol. 58 (2008) 1687–1692.
[15] Y.H. Song, P. Yuan, B.H. Zheng, J. Peng, F. Yuan, Y. Gao, Nutrients removal and recovery by crystallization of magnesium ammonium phosphate from synthetic swine wastewater, Chemosphere 69 (2007) 319–324.
[16] D. Crutchick, J.M. Garrido, Kinetics of the reversible reaction of struvite crystallisation, Chemosphere 154 (2016) 567–572.
[17] H. Saidou, S.B. Moussa, M.B. Amor, Influence of air flow rate and substrate nature on heterogeneous struvite precipitation, Environ. Technol. 30 (2009) 75–83.
[18] B. Bergmans, Struvite Recovery from Digested Sludge at WWTP West, Masters Thesis, Faculty of Civil Engineering and Geosciences, Delft University of Technology, Delft, the Netherlands, 2011.
[19] A. Andrade, R.D. Schuiling, The chemistry of struvite crystallization, *Mineralogy Journal* (Ukraine) 23 (5/6) (2001) 37–46.
[20] M.I. Ali, P.A. Schneider, A fed-batch design approach of struvite precipitation in controlled supersaturation, Chem. Eng. Sci. 61 (2006) 3951–3961.
[21] A.N. Kofina, K.D. Demadis, P.G. Koutsoukos, The effect of citrate and phosphocitrate on struvite spontaneous precipitation, Cryst. Growth Des. 7 (12) (2007) 2705–2712.
[22] I. Kabdasli, Z. Atalay, Ö. Tunay, Effect of solution composition on struvite crystallization, J. Chem. Technol. Biotechnol. 12 (2017) 2921–2928.
[23] Y. Song, Y. Dai, Q. Hu, X. Yu, F. Qian, Effects of three kinds of organic acids on phosphorus recovery by magnesium ammonium phosphate (MAP) crystallization from synthetic swine wastewater, Chemosphere 101 (2014) 41–48.
[24] A.P. Bayuseno, W.W. Schmahl, Characterisation of MSWI fly ash through mineralogy and water extraction, Resour. Conserv. Recycl. 55 (2011) 524–534.
[25] H.M. Rietveld, A profile refinement method for nuclear and magnetic structures, J. Appl. Crystallogr. 2 (1969) 65–71.
[26] J. Rodriguez-Carvajal, Program Fullprof.2k, Version 3.30, Laboratoire Leon Brillouin, France, June 2005.
[27] G. Caglioti, A. Paoletti, F.P. Ricci, Choice of collimator for a crystal spectrometer for neutron diffraction, Nucl. Instrum. 35 (1958) 223–228.
[28] R.J. Hill, C.J. Howard, Quantitative phase analysis from neutron powder diffraction data using the Rietveld method, J. Appl. Crystallogr. 20 (1987) 467–474.
[29] P.-Y. Mahieux, J.-E. Aubert, M. Cyr, M. Coutand, B. Husson, Quantitative mineralogical composition of complex mineral wastes–contribution of the Rietveld method, Waste Manag. 30 (2010) 378–388.
[30] K.S. Le Corre, Understanding Struvite Crystallization and Recovery. PhD Thesis, Cranfield University, UK, 2006, pp. 72–73.
[31] K.N. Ohlinger, T.M. Young, E.D. Schroeder, Postdigestion struvite precipitation using a fluidized bed reactor, J. Environ. Eng. 126 (2000) 361–368.
[32] M. Quintana, E. Sanchez, M.F. Colmenarejo, J. Barrera, G. Garcia, R. Borja, Kinetics of phosphorus removal and struvite formation by the utilization of by-product of magnesium oxide production, Chem. Eng. J. 111 (2005) 45–52.
[33] M.S. Rahaman, D.S. Mavinic, N. Ellis, Effects of various process parameters on struvite precipitation kinetics and subsequent determination of rate constants, Water Sci. Technol. 57 (2008) 647–654.
[34] M.L. Harrison, M.R. Johns, E.T. White, C.M. Mehta, Growth rate kinetics for struvite crystallisation, Chem. Eng. Trans. 25 (2011) 309–314.
[35] Ch.N. Bouropoulos, P.G. Koutsoukos, Spontaneous precipitation of struvite from aqueous solutions, J. Cryst. Growth 213 (2000) 381–388.
[36] T. Zhang, L. Ding, H. Ren, Pretreatment of ammonium removal from landfill leachate by chemical precipitation, J. Hazard Mater. 166 (2009) 911–915.
[37] K.S. Le Corre, E.V. Jones, P. Hobbs, S.A. Parsons, Phosphorus recovery from wastewater by struvite crystallization: a review, Crit. Rev. Environ. Sci. Technol. 39 (2009) 433–477.
[38] K.S. Le Corre, E.V. Jones, P. Hobbs, S.A. Parsons, Impact of calcium on struvite crystal size, shape and purity, J. Cryst. Growth 283 (2005) 514–522.
[39] A.P. Bayuseno, W.W. Schmahl, Hydrothermal synthesis of struvite and its phase transition: Impacts of pH, heating and subsequent cooling methods, J. Cryst. Growth 498 (2018) 336–345.
[40] M.I.H. Bhuiyan, D.S. Mavinic, F.A. Koch, Thermal decomposition of struvite and its phase transition, Chemosphere 70 (2008) 1347–1356.
[41] A. Capdevielle, E. Sykorová, B. Biscans, F. Bélinea, M.-L. Daumer, Optimization of struvite precipitation in synthetic biologically treated swine wastewater-Determination of the optimal process parameters, J. Hazard Mater. 244–245 (2013) 357–369.
[42] J.D. Doyle, S.A. Parsons, Struvite formation, control and recovery, Water Res. 36 (2002) 3925–3940.
[43] M.T. Munir, B. Li, I. Boiarkina, S. Baroutian, W. Yu, B.R. Young, Phosphate recovery from hydrothermally treated sewage sludge using struvite precipitation, Bioresour. Technol. 239 (2017) 171–179.
[44] A. Korchef, H. Saidou, M.B. Amor, Phosphate recovery through struvite precipitation by CO_2 removal: effect of magnesium, phosphate and ammonium concentrations, J. Hazard. Mater. 186 (2011) 602–613.

Kinetics and morphological characteristics of struvite (MgNH4PO4.6H2O) under the influence of maleic acid

ORIGINALITY REPORT

12%	8%	7%	3%
SIMILARITY INDEX	INTERNET SOURCES	PUBLICATIONS	STUDENT PAPERS

PRIMARY SOURCES

1	sphinxsai.com Internet Source	1%
2	"Effects of Metal Oxides on the Crystallization of BaSo4 in a Vibrated Batch Crystallizer System", International Journal of Engineering and Advanced Technology, 2020 Publication	1%
3	Atif Muhmood, Xiqing Wang, Renjie Dong, Shubiao Wu. "New insights into interactions of organic substances in poultry slurry with struvite formation: An overestimated concern?", Science of The Total Environment, 2021 Publication	1%
4	echoexcelsia.weebly.com Internet Source	1%
5	rasayanjournal.co.in Internet Source	1%

6	Quintana, M.. "Kinetics of phosphorus removal and struvite formation by the utilization of by-product of magnesium oxide production", Chemical Engineering Journal, 20050701 Publication	1 %
7	www.nature.com Internet Source	1 %
8	ghorannevis.com Internet Source	<1 %
9	www.science.gov Internet Source	<1 %
10	findresearcher.sdu.dk Internet Source	<1 %
11	Submitted to University of Leeds Student Paper	<1 %
12	A.P. Bayuseno, W.W. Schmahl. "Hydrothermal synthesis of struvite and its phase transition: impacts of pH, heating and subsequent cooling methods", Journal of Crystal Growth, 2018 Publication	<1 %
13	dokumen.pub Internet Source	<1 %
14	jultika.oulu.fi Internet Source	<1 %

15	www.matec-conferences.org Internet Source	<1 %
16	aip.scitation.org Internet Source	<1 %
17	pubs.rsc.org Internet Source	<1 %
18	open.library.ubc.ca Internet Source	<1 %
19	s3-eu-west-1.amazonaws.com Internet Source	<1 %
20	Submitted to CSU, San Jose State University Student Paper	<1 %
21	D. Crutchik, J.M. Garrido. "Kinetics of the reversible reaction of struvite crystallisation", Chemosphere, 2016 Publication	<1 %
22	www.orientjchem.org Internet Source	<1 %
23	biotechnologyforbiofuels.biomedcentral.com Internet Source	<1 %
24	Athanasius P. Bayuseno, Wolfgang W. Schmahl. "Crystallization of struvite in a hydrothermal solution with and without calcium and carbonate ions", Chemosphere, 2020	<1 %

Publication

25	Zhang, Yanyang, Weixian Zhang, and Bingcai Pan. "Struvite-based phosphorus recovery from the concentrated bioeffluent by using HFO nanocomposite adsorption: Effect of solution chemistry", Chemosphere, 2015. Publication	<1 %
26	dspace.lib.cranfield.ac.uk Internet Source	<1 %
27	whattowriteaboutinaresearchpaper.blogspot.com Internet Source	<1 %
28	worldwidescience.org Internet Source	<1 %
29	Atef Korchef, Hassidou Saidou, Mohamed Ben Amor. "Phosphate recovery through struvite precipitation by CO2 removal: Effect of magnesium, phosphate and ammonium concentrations", Journal of Hazardous Materials, 2011 Publication	<1 %
30	K. S. Le Corre, E. Valsami-Jones, P. Hobbs, S. A. Parsons. "Phosphorus Recovery from Wastewater by Struvite Crystallization: A Review", Critical Reviews in Environmental Science and Technology, 2009 Publication	<1 %

eprints.nottingham.ac.uk

31	Internet Source	<1%
32	eprints.utar.edu.my Internet Source	<1%
33	etheses.whiterose.ac.uk Internet Source	<1%
34	www.scielo.org.co Internet Source	<1%
35	Yonghui Song, Yunrong Dai, Qiong Hu, Xiaohua Yu, Feng Qian. "Effects of three kinds of organic acids on phosphorus recovery by magnesium ammonium phosphate (MAP) crystallization from synthetic swine wastewater", Chemosphere, 2014 Publication	<1%

Exclude quotes	Off	Exclude matches	Off
Exclude bibliography	On		

Kinetics and morphological characteristics of struvite (MgNH4PO4.6H2O) under the influence of maleic acid

GRADEMARK REPORT

FINAL GRADE

/0

GENERAL COMMENTS

Instructor

PAGE 1

PAGE 2

PAGE 3

PAGE 4

PAGE 5

PAGE 6

PAGE 7

PAGE 8

PAGE 9